ACS APPLIED MATERIALS & INTERFACES

Letter

www.acsami.org

Facile Fabrication of TiO_2–Graphene Composite with Enhanced Photovoltaic and Photocatalytic Properties by Electrospinning

Zhu Peining,[†,‡] A. Sreekumaran Nair,*[,‡] Peng Shengjie,[‡] Yang Shengyuan,[‡] and Seeram Ramakrishna[†,‡]

[†]Department of Mechanical Engineering, National University of Singapore, Singapore, 117574, Singapore

[‡]Healthcare and Energy Materials Laboratory, Nanoscience and Nanotechnology Initiative, National University of Singapore, 117581, Singapore

Supporting Information

ABSTRACT: We report the fabrication of one-dimensional TiO_2–graphene nanocomposite by a facile and one-step method of electrospinning. The unique nanostructured composite showed a significant enhancement in the photovoltaic and photocatalytic properties in comparison to TiO_2 as demonstrated in dye-sensitized solar cells and photodegradation of methyl orange.

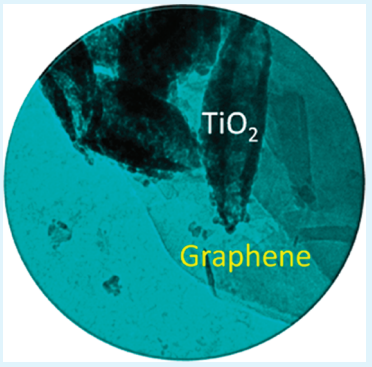

KEYWORDS: *electrospinning, TiO_2–graphene composite, dye-sensitized solar cells, photocatalysis, one-dimensional mesostructures*

Graphene, a two-dimensional nanomaterial, is attracting widespread attention because of its remarkable properties such as superior mechanical strength,[1] excellent mobility of charge carriers,[2] high thermal conductivity,[3] and large specific surface area.[4] Graphene and its composites[5] found applications in fields such as photocatalysis,[6] liquid crystal displays,[7] lithium-ion batteries,[8−10] and solar cells.[11−13] Integration of graphene into materials such as metal oxides and polymers render them unique functionalities.[14] For example, solar cells with layered graphene/quantum dots and graphene/TiO_x/quantum dots have been demonstrated to have good performances due to the ability of graphene in enhancing charge collection and transport.[15,16] The extended light absorption range as well as the improved charge separation caused by the incorporation of graphene into TiO_2 have been attributed to the enhanced photocatalysis performance.[6,17]

Among the graphene-based composites, TiO_2–graphene composites (TGCs) have been widely studied for various applications. TGCs with enhanced performance in lithium-ion batteries,[8−10] solar cells,[12,18] and photocatalysis[19−25] have been reported. So far, TiO_2–graphene composites (TGCs) have been fabricated by the methods of hydrothermal method,[12,26] molecular grafting,[11] solvothermal method,[10] and heterogeneous coagulation.[13] However, most of the TiO_2–graphene composites reported have been fabricated with complicated processes involving hydrothermal treatments, assembly of graphene with TiO_2 by multistep methods, or the reduction of the TiO_2-graphene oxide composite into TiO_2-graphene composite.[12,20,27] For photovoltaic and photocatalysis applications, TiO_2 in one-dimensional (1D) morphology is desired compared to the spherical TiO_2 nanoparticles owing to excellent mobility of charge carriers,[28] high surface areas,[29] scattering more light at the red part of the solar spectrum,[30] and the existence of straight pores which enhance the accessibility of electrodes to the hole transporting materials[31] and hence enhanced charge collection and transport.[32,33] There were only a few reports on TGCs with 1D TiO_2; however, these employed graphitic oxide (GO).[19] Thus it is desirable to develop a simple method to integrate graphene into 1D nanostructured TiO_2 for enhanced photovoltaics and photocatalytic applications.

In this letter, we report for the first time a simple method to fabricate TGCs by electrospinning. Electrospinning is a simple and cost-effective technique to fabricate 1D nanostructures in random and aligned, core/shell and hollow configurations.[34,35] Besides the traditional 1D nanostructures of nanofibers/nanowires, we have recently shown that a novel 1-D rice-shaped TiO_2 mesostructures with single crystallinity and high surface area could also be fabricated by electrospinning.[36,37] The unique mesostructures showed better photocatalytic and photovoltaic properties than the commercial P-25 TiO_2 and electrospun TiO_2 nanofibers. In the present case, by the introduction of cetyltrimethylammonium bromide (CTAB)-functionalized DMF soluble graphene[38,39] (see the Supporting

Received: October 20, 2011
Accepted: January 31, 2012
Published: January 31, 2012

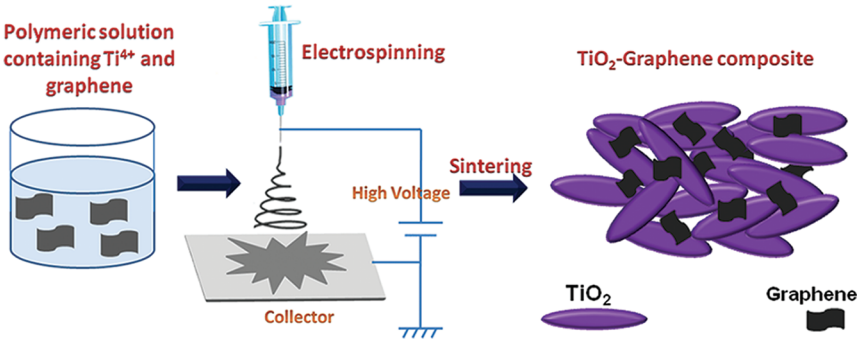

Figure 1. Schematic of the fabrication of TGCs by electrospinning. A polymeric solution consisting of PVAc, dispersed graphene, acetic acid, and TiO_2 precursor was electrospun to get a nanofiber mat that was subsequently sintered at 450 °C for 1 h to obtain the 1D TGC.

Information, SI-1 and SI-2 for synthesis and characterization of graphene) into the polymeric solution for electrospinning, we have successfully integrated graphene into the TiO_2. The obtained composites displayed enhanced photovoltaic and photocatalytic properties compared to bare TiO_2 (rice grain-shaped TiO_2) as demonstrated in the applications of dye-sensitized solar cells (DSCs) and photocatalytic degradation of methyl orange (MO).

The synthesis procedure is presented in a schematic in Figure 1. Briefly, 0.6 mg offunctionalized graphene[38] was dissolved in *N*,*N*-dimethyl acetamide containing polyvinyl acetate (PVAc), acetic acid, and a titanium precursor and subjected to electrospinning. The collected PVAc−TiO_2−graphene composite fibers were sintered at 450 °C for 1 h to obtain the TGC (see the Supporting Information, SI-3). Figure 2 A shows the

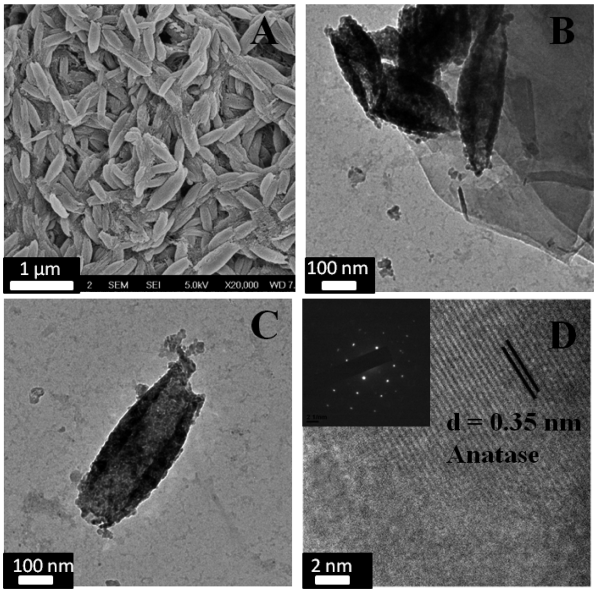

Figure 2. (A) SEM and (B) TEM image of TiO_2−graphene composite (TGC). (C) TEM and (D) lattice-resolved image of a single TGC. Inset of D shows an SAED pattern showing the single crystallinity of the TiO_2.

SEM image of the TGC obtained after sintering. A well-connected TGC network with randomly distributed rice grain-shaped 1D TiO_2 mesostructures could be seen in the SEM image. The average dimension of the TGC mesostructures was ∼450 nm in length and ∼150 nm in diameter. Graphene was not directly spotted in the SEM image as this might be submerged into the TiO_2 network (as the amount of the former being small in comparison to the latter). The composite was further investigated by TEM. The TEM image (Figure 2B) shows the presence of exfoliated graphene flakes and the TiO_2 forming a composite. The TEM image of a single rice-like mesostructure (Figure 2C) clearly shows that the same was composed of small spherical particles with an average diameter of ∼20 nm, which leads to a relatively high surface area of ∼62 m^2/g for the composite. Figure 2D shows the lattice-resolved image and the SAED pattern of the TiO_2 in the composite, indicating its single crystalline anatase phase with the perfect lattice spacing of 0.35 nm [(101) anatase]. This is in agreement with the results of the XRD pattern shown in Figure 3A. The

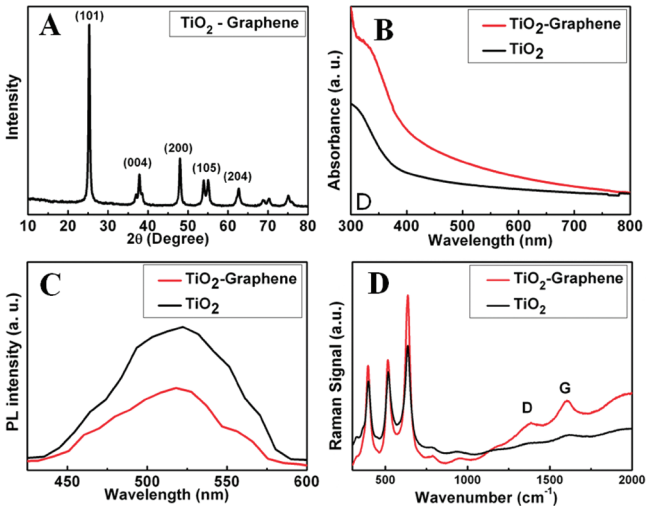

Figure 3. (A) XRD pattern, (B) UV−vis spectra, (C) photoluminescence (PL) spectra, and (D) Raman spectra of the TiO_2 and the TGC.

peaks in the XRD pattern clearly show the (101), (004), (200), and (105) lattice planes of the anatase TiO_2. The diffraction peak of graphene was not separately seen as the same at ∼25° (002) overlaps with the (101) diffraction of TiO_2.[9]

The TGC was further characterized by the UV−vis absorption spectroscopy and photoluminescence (PL) spectroscopy, respectively. From the UV−vis spectra (Figure 3B), we can see that the spectrum of TiO_2 underwent a red-shift of 25 nm with the incorporation of graphene indicating the interaction between the TiO_2 and the graphene.[6,20] The enhanced absorption in the visible- and near-IR regions due to the incorporation of graphene into TiO_2 would be beneficial

dx.doi.org/10.1021/am201448p | *ACS Appl. Mater. Interfaces* 2012, 4, 581−585

for photovoltaics and photocatalysis applications of TiO_2.[6] The PL spectra of the TiO_2 and the TGC excited at 375 nm are presented in Figure 3C. The emission peak of TiO_2 at around 510 nm was slightly broadened and quenched in intensity indicating electron transfer from the conduction band of TiO_2 to the graphene.[19] This corresponds to an efficient charge separation in the TGC, which would have an effect on the photovoltaic and photocatalytic properties of the material. Raman spectrum of TGC showed the presence of D and G bands of graphene indicating successful incorporation of the same into the TiO_2 matrix (Figure 3D). In comparison to the functionalized graphene (see the Supporting Information, SI-2), the increased I_D/I_G peak intensity ratio in the TGC reveals the presence of increased defects and disorders of graphene introduced by the integration process demonstrating the strong interaction between the TiO_2 and graphene.[39]

The TGC was utilized in the active layer for DSCs. The DSCs were fabricated by doctor-blading as reported previously (see the Supporting Information, SI-3).[36] The working area of the cells was 0.25 cm^2 and the thickness of the electrodes was ~11 μm (this was found to be the optimized thickness of the electrode from several experimental trials, see inset in Figure 4A

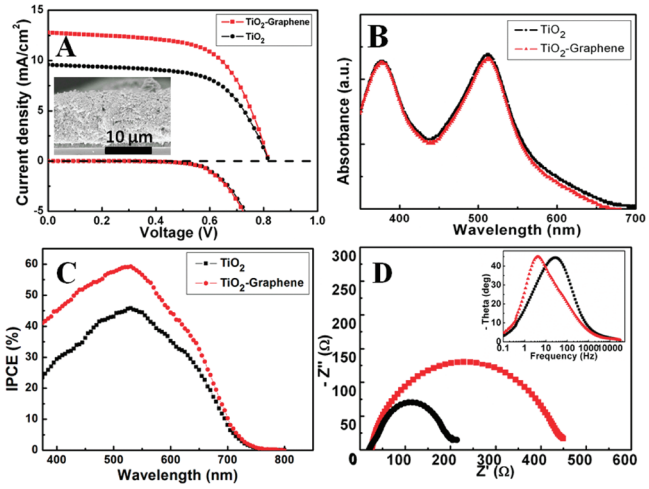

Figure 4. (A) $I-V$ parameters (photocurrent and dark current), (B) UV–visible spectra of the detached dye molecules, (C) IPCE spectra, and (D) the EIS spectra of the different electrodes. The inset in A shows the cross-sectional SEM image of the electrode.

for the cross-sectional SEM image of the electrode and the Supporting Information, SI-4, for thickness-dependent photovoltaic parameters). To study the effect of the graphene concentration on the performance of solar cells, TGCs with different concentrations (0.25–0.75 wt % graphene with respect to TiO_2) were fabricated and made into electrodes, it has been found that the 0.5 wt % was the optimum concentration to have the better device performance (see the Supporting Information, SI-5). The short circuit current density–voltage ($J_{sc}-V$) response is presented in Figure 4A showing improved energy conversion efficiency of the TGC electrode (0.5 wt %). With the introduction of the graphene into the TiO_2 network, the J_{sc} has been improved from 9.58 to 12.78 mA/cm^2 while maintaining the high open-circuit voltage at 0.82 V and the fill-factor remained at ~62%. Hence, the overall energy conversion efficiency was enhanced from 4.89 to 6.49%, which is a 33% enhancement. The dark current (arises mainly from the recombination of charge carriers by the reduction of I_3^- at the TiO_2 surfaces) characteristics were also measured. It is evident that the incorporation of graphene did not affect the dark current–voltage characteristics of the electrodes much and both the electrodes showed nearly the similar diode effect.[40] Graphene being a zero band material,[41] its calculated work function is close to that of FTO (−4.22 eV vs −4.4 eV for FTO) and therefore the apparent Fermi level of TiO_2 was not affected by the incorporation of graphene. This is the reason why the V_{oc} was unaffected which makes graphene a superior candidate for photovoltaics over CNTs.[12] The dye-loading in TGC and TiO_2 electrodes of similar thicknesses were 1.57×10^{-7} mol/cm^2 and 1.62×10^{-7} mol/cm^2, respectively (the UV–visible spectra of the dyes desorbed from the TiO_2 electrodes are given in Figure 4B). The slightly reduced dye-loading for the TGC could be attributed to the reduced effective mass of the TiO_2. Thus, it is obvious that despite the effective reduction in the amount of dyes, the TGC showed superior photovoltaic parameters because of a strong role played by the graphene in the composite. The increase in J_{sc} with the incorporation of graphene could be attributed to the effective charge separation and the resultant suppression of recombination of the excited electrons with the oxidized dye and the redox electrolyte (as evidenced from the PL spectra) as well as the enhanced charge transport through the TGC network. This is further evident from the incident photon-to-current conversion efficiency (IPCE) spectra shown in Figure 4C. With nearly similar dye-loadings in TiO_2 and TGC, the IPCE peak of the TGC was ~31% (from 45% to 59%) higher than that of the TiO_2. As is well-known, the most important factors affecting the IPCE are the light harvesting efficiency, and charge separation and collection yields.[42] As the contribution from the first parameter is negligible in the present case because of nearly similar dye-loadings, it becomes obvious that the 31% IPCE enhancement was mainly due to the contribution from the latter two parameters *viz.* the enhanced charge separation (as reflected in the PL spectra) and faster charge transport and collection (see the electrochemical impedance, EIS, data below). To get further insights on the enhanced photovoltaic parameters of the TGCs, we collected electrochemical impedance spectra (EIS). Figure 4D shows the EIS of the cells measured at a bias voltage of 0.70 V under dark, demonstrating the same results with the PL spectra. The large semicircle at the intermediate frequency that corresponds to the charge recombination resistance at the TiO_2/dye/electrolyte interface[43,44] indicates that the charge recombination was highly retarded by the incorporation of graphene into the TiO_2 network, because of a more effective charge separation (and transport) process through the TGC network. This is further evident from the bode-phase plots shown in the inset of Figure 4B. With the integration of graphene, the characteristic frequency peak of the composite (which is related to the inverse of recombination time or electron lifetime[13] in the TGC matrix) shifted to lower frequency, indicating reduced recombinations and longer electron lifetime.

The enhanced photocatalytic property of the composite was deducted from the photodegradation of MO (see the Supporting Information, SI-3). Among the above three compositions of TGC, the one with 0.75 wt % graphene showed the highest photocatalytic activity which could be because of the enhanced adsorption of MO on the TGC. The UV–visible spectra and a chart showing the concentration of MO remaining after 3 h of UV-light irradiation are presented in panels A and B in Figure 5, respectively. The typical absorption

dx.doi.org/10.1021/am201448p | ACS Appl. Mater. Interfaces 2012, 4, 581–585

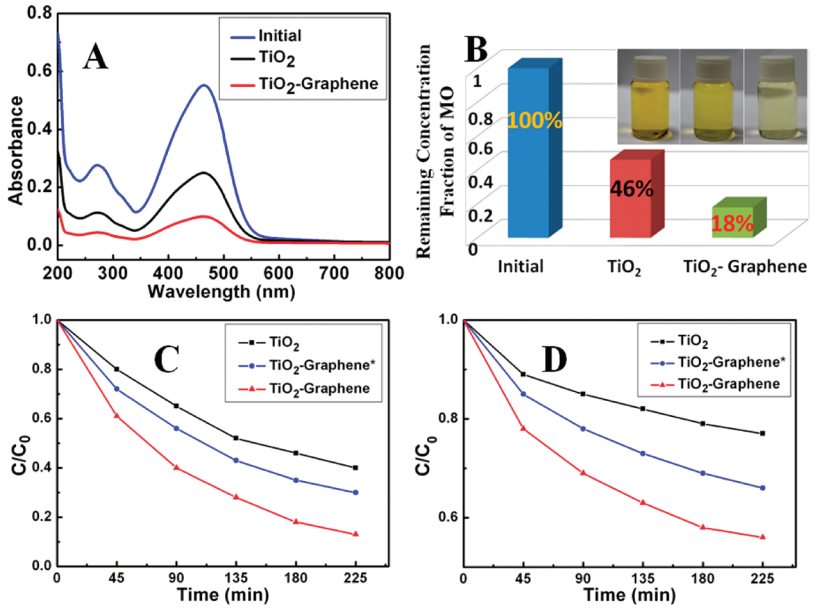

Figure 5. (a) UV−visible spectra and (b) bar plotting of initial dye solutions and the dye solutions after 3 h irradiation in UV light. Photodegradation of dye solutions under (a) UV light and (b) visible light (>400 nm). TiO_2−graphene* denotes the physical mixture of TiO_2 and graphene obtained by mechanical grinding.

feature of MO (aq. solution) at 460 nm decreased in intensity after irradiation with TiO_2 and TGC, respectively, indicating the photodegradation of MO. The enhanced photodegradation by the composite was clearly visible from the spectra and the chart. The concentration of MO remaining after irradiation was 18% in the case of TGC and 46% in the case of TiO_2. The digital photographs were also presented to provide a visual evidence for the enhanced photodegradation (inset of Figure 5B) by the TGC. The TGC material was found to be reusable several times just after sintering at 250 °C. For a comparison of the photocatalytic properties, we have also collected data from a TGC obtained by physical mixing of TiO_2 and graphene (by grinding, denoted as TiO_2−graphene* in panels C and D in Figure 5). The systematic data of the photodegradation by the TiO_2, TiO_2-graphene*, and the electrospun TGC (0.75 wt %) under the UV and visible irradiations were plotted in panels C and D in Figure 5, respectively. The better performance shown by the electrospun TGC in both the cases demonstrates better percolation of graphene into the TiO_2 matrix thus detailing the usefulness of the electrospinning process for the fabrication of the composite. The mechanical mixing of TiO_2 and the graphene may not produce a composite with well-dispersed graphene in TiO_2. The reason for the improved photocatalysis could be traced to the enhanced adsorptivity (see the Supporting Information, SI-6, for the amount of dye molecules remaining in solution after equilibration in the dark for 10 min), the extended light absorption range (as evident from the UV−vis spectra in Figure 3), and the enhanced charge separation and transport (as evident from the PL and EIS spectra in Figure 3). The visible-light-assisted photocatalysis (though less efficient than the UV light assisted in the present case as the TGC is still TiO_2-rich) by the TGC is promising from the perspective of environmental remediation.

In summary, we have fabricated TiO_2−graphene composite by a facile process of electrospinning. The TGC in which the TiO_2 was single crystalline has shown enhanced photovoltaic and photocatalytic properties as demonstrated in DSCs and photodegradation of MO. We believe that the simple one-step approach to fabricate TGC with the unique morphology would open up many windows for further applications of the material in Li-ion batteries, photoelectrochemical water splitting, sensors, etc.

■ ASSOCIATED CONTENT

Ⓢ Supporting Information

Experimental detail, Raman spectrum of graphene, *I*−*V* characteristics of electrodes with different thickness and different graphene concentration, and the plots of remaining concentration of dye molecules after equilibrium. This material is available free of charge via the Internet at http://pubs.acs.org.

■ AUTHOR INFORMATION

Corresponding Author

*E-mail: nniansn@nus.edu.sg (A.S.N.); seeram@nus.edu.sg (S.R.).

■ ACKNOWLEDGMENTS

The authors thank National Research Foundation and M3TC (EDB), Singapore for financial support (Grants NRF 2007 EWT-CERP 01-0531 and R-261-501-018-414).

■ REFERENCES

(1) Lee, C.; Wei, X. D.; Kysar, J. W.; Hone, J. *Science* **2008**, *321*, 385.
(2) Bolotin, K. I.; Sikes, K. J.; Jiang, Z.; Klima, M.; Fudenberg, G.; Hone, J.; Kim, P.; Stormer, H. L. *Solid State Commun.* **2008**, *146*, 351.
(3) Balandin, A. A.; Ghosh, S.; Bao, W. Z.; Calizo, I.; Teweldebrhan, D.; Miao, F.; Lau, C. N. *Nano Lett.* **2008**, *8*, 902.
(4) McAllister, M. J.; Li, J. L.; Adamson, D. H.; Schniepp, H. C.; Abdala, A. A.; Liu, J.; Herrera-Alonso, M.; Milius, D. L.; Car, R.; Prud'homme, R. K.; Aksay, I. A. *Chem. Mater.* **2007**, *19*, 4396.
(5) Stankovich, S.; Dikin, D.; Dommett, G.; Kohlhaas, K.; Zimney, E.; Stach, E.; Piner, R.; Nguyen, S.; Ruoff, R. *Nature* **2006**, *442*, 282.
(6) Zhang, H.; Lv, X.; Li, Y.; Wang, Y.; Li, J. *ACS Nano* **2009**, *4*, 380.
(7) Blake, P.; Brimicombe, P.; Nair, R.; Booth, T.; Jiang, D.; Schedin, F.; Ponomarenko, L.; Morozov, S.; Gleeson, H.; Hill, E. *Nano Lett.* **2008**, *8*, 1704.

(8) Wang, D.; Choi, D.; Li, J.; Yang, Z.; Nie, Z.; Kou, R.; Hu, D.; Wang, C.; Saraf, L.; Zhang, J. *ACS Nano* **2009**, *3*, 907.
(9) Chen, J. S.; Wang, Z.; Dong, X. C.; Chen, P.; Lou, X. W. D. *Nanoscale* **2011**, *3*, 2158.
(10) Ding, S.; Chen, J. S.; Luan, D.; Boey, F. Y. C.; Madhavi, S.; Lou, X. W. D. *Chem. Commun.* **2011**, *47*, 5780.
(11) Tang, Y.; Lee, C.; Xu, J.; Liu, Z.; Chen, Z.; He, Z.; Cao, Y.; Yuan, G.; Song, H.; Chen, L. *ACS Nano* **2010**, *4*, 3482.
(12) Yang, N.; Zhai, J.; Wang, D.; Chen, Y.; Jiang, L. *ACS Nano* **2010**, *4*, 887.
(13) Sun, S.; Gao, L.; Liu, Y. *Appl. Phys. Lett.* **2010**, *96*, 083113.
(14) Stankovich, S.; Dikin, D. A.; Dommett, G. H. B.; Kohlhaas, K. M.; Zimney, E. J.; Stach, E. A.; Piner, R. D.; Nguyen, S. B. T.; Ruoff, R. S. *Nature* **2006**, *442*, 282−286.
(15) Yang, H. B.; Guo, C. X.; Guai, H. G.; Song, Q. L.; Jiang, S. P.; Li, C. M. *ACS Appl. Mater. Interfaces* **2011**, *3*, 1940.
(16) Guo, C. X.; Yang, H. B.; Sheng, Z. M.; Lu, Z. S.; Song, Q. L.; Li, C. M. *Angew. Chem., Int. Ed.* **2010**, *49*, 3014.
(17) Kamat, P. V. *J. Phys. Chem. Lett.* **2011**, *2*, 242.
(18) Ng, Y. H.; Lightcap, I. V.; Goodwin, K.; Matsumura, M.; Kamat, P. V. *J. Phys. Chem. Lett.* **2010**, *1*, 2222.
(19) Liu, J.; Bai, H.; Wang, Y.; Liu, Z.; Zhang, X.; Sun, D. *Adv. Func. Mater.* **2010**, *20*, 4175.
(20) Peng, W.; Wang, Z.; Yoshizawa, N.; Hatori, H.; Hirotsu, T.; Miyazawa, K. *J. Mater. Chem.* **2010**, *20*, 2424.
(21) Zhang, H.; Xu, P.; Du., G.; Chen, Z.; Oh, K.; Pan, D.; Jiao, Z. *Nano Research* **2011**, *4*, 274.
(22) Zhang, Y.; Tang, Z. R.; Fu, X.; Xu, Y. J. *ACS Nano* **2010**, *4*, 7303.
(23) Zhang, X. Y.; Li, H. P.; Cui, X. L.; Lin, Y. *J. Mater. Chem.* **2010**, *20*, 2801.
(24) Jiang, B.; Tian, C.; Pan, Q.; Jiang, Z.; Wang, J. Q.; Yan, W.; Fu, H. *J. Phys. Chem. C* **2011**, *115*, 23718.
(25) Zhou, K.; Zhu, Y.; Yang, X.; Jiang, X.; Li, C. *New J. Chem.* **2011**, *35*, 353.
(26) Li, N.; Liu, G.; Zhen, C.; Li, F.; Zhang, L.; Cheng, H. M. *Adv. Funct. Mater.* **2011**, *21*, 1717.
(27) Fan, W.; Lai, Q.; Zhang, Q.; Wang, Y. *J. Phys. Chem. C* **2011**, *115*, 10694.
(28) Feng, X.; Shankar, K.; Varghese, O. K.; Paulose, M.; Latempa, T. J.; Grimes, C. A. *Nano Lett.* **2008**, *8*, 3781.
(29) Tian, Z. R.; Voigt, J. A.; Liu, J.; Mckenzie, B.; Xu, H. *J. Am. Chem. Soc.* **2003**, *125*, 12384.
(30) Tan, B.; Wu, Y. *J. Phys. Chem. B* **2006**, *110*, 15932.
(31) Song, M. Y.; Kim, D. K.; Jo, S. M.; Kim, D. Y. *Synth. Met.* **2005**, *155*, 635.
(32) Zhu, K.; Neale, N. R.; Miedaner, A.; Frank, A. J. *Nano Lett.* **2007**, *7*, 69.
(33) Mor, G. K.; Shankar, K.; Paulose, M.; Varghese, O. K.; Grimes, C. A. *Nano Lett.* **2006**, *6*, 215.
(34) Li, D.; Xia, Y. *Adv. Mater.* **2004**, *16*, 1151.
(35) Ramakrishna, S.; Jose, R.; Archana, P. S.; Nair, A. S.; Balamurugan, R.; Venugopal, J.; Teo, W. E. *J. Mater. Sci.* **2010**, *45*, 6283.
(36) Yang, S.; Zhu, P.; Nair, A. S.; Ramakrishna, S. *J. Mater. Chem.* **2011**, *21*, 6541.
(37) Nair, A. S.; Shengyuan, Y.; Peining, Z.; Ramakrishna, C. *Chem. Commun.* **2010**, *46*, 7421.
(38) Vadukumpully, S.; Gupta, J.; Zhang, Y.; Xu, G. U.; Valiyaveettil, S. *Nanoscale* **2011**, *3*, 303.
(39) Vadukumpully, S.; Gupta, J.; Valiyaveettil, S. *Carbon* **2009**, *47*, 3288.
(40) Yang, H. B.; Guai, H. G.; Guo, C. X.; Song, Q. L.; Jiang, S. P.; Wang, Y. L.; Zhang, W.; Li, C. M. *J. Phys. Chem. C* **2011**, *115*, 12209.
(41) Freitage, M. *Nat. Nanotechnol.* **2008**, *3*, 455.
(42) Grätzel, M. *Inorg. Chem.* **2005**, *44*, 6841.
(43) Wang, Q.; Moser, J. E.; Grätzel, M. *J. Phys. Chem. B* **2005**, *109*, 14945.
(44) Peining, Z.; Nair, A. S.; Shenyuan, Y.; Shengjie, P.; Kumar, E. N.; Ramakrishna, S. *Photochem. Photobiol. A* **2012**, DOI: 10.1016/j.photochem.2012.01.002.